ISSN 2347 - 3983
Volume 9. No. 3, March 2021
International Journal of Emerging Trends in Engineering Research
Available Online at http://www.warse.org/IJETER/static/pdf/file/ijeter23932021.pdf
https://doi.org/10.30534/ijeter/2021/23932021

Inhibition of Calcium-dependent Protein Kinase 1 from *Cryptosporidium parvum*: An In-Silico Approach from Protein Modelling to Lead Compounds Identification for Cryptosporidiosis Treatment

Kalpana[a]*, R.K. Srivastava[b], Ravindra Nath[c]
[a]Department of Biotechnology, Dr. Ambedkar Institute of Technology for Handicapped, Kanpur, India-208024;kalpna@aith.ac.in
[b]Rural Division Extension, Central Institute for Medicinal and Aromatic Plant, Lucknow, India-206015;rksrivastava@cimap.res.in
[c]University Institute of Engineering and Technology, CSJM University, Kanpur, India-208024; rnkatiyar@gmail.com
*Corresponding author

ABSTRACT

Background: A year into the pandemic and there are still so many unknowns. There are very few specific answers about the origin of the virus, but this much is clear. It is not the last pandemic we will face, and far more dangerous pandemics await us in the future.Cryptosporidiosis can produce major epidemics whenever public health measures fails.Human cryptosporidiosis is a diarrheal disease mainly propagated by *Cryptosporidium parvum* (*C. parvum*) and *Cryptosporidium hominis* (*C. hominis*). It is a self-limited illness in immunocompetent patients but become a severe life-threatening illness in immunocompromised patients and children under five year of age. Several studies have explored the effects of cryptosporidiosis on the mortality rate of younger children. According to one research, about globally 30-50 % death of children of five years occurs due to cryptosporidiosisand is a second primary infection in 12-13 months toddlers related with fatality. Although many attempts have been made to address this issue,it still lacks effective treatment options. The Nitazoxanide drug has shown moderate efficacy in immunocompetent patients.

Methods:in this research study, we developed a model of CpCDK1 protein and then proposes a workflow for the identification and prioritization of potential lead compounds against CpCDK1 protein.To achieve the objective, a high-throughput virtual screening,molecular dynamics, and pharmacokinetics analysis of selected hits were performed.

Results: The best-chosen protein model was analyzed and plot, and VADAR analysis.Then molecular docking analysis was performed for virtual screening of lead-like subset of ZINC database and binding interaction characterization.

Conclusion: This study's research finding may contribute to discovering potential CpCDK1 inhibitors that are favorable selective for their binding sites. These 'lead' compounds may act as a starting point for designing anti-cryptosporidial agents.

Key words: Cryptosporidiosis; CADD;Molecular docking;COVID-19; Protein Kinases.

1.INTRODUCTION

Cryptosporidiosis is a gastrointestinal illness caused by the intracellular protozoan parasite *Cryptosporidium* species (Spp.). Human cryptosporidiosis was first reported in 1976. It is a definitive 'emerging diarrheal disease. It has an extremely low infection dose[1]. The impact of the disease is most severe in immunocompromised individuals. It is wellresilient to anti-parasitic therapy. It has human and non-human reservoirs. Cryptosporidiosis is the leading cause of diarrhea in developing nations and younger children[2]. Cryptosporidiosis is a recurrent reason for mortality in AIDS patients. It has been documented that children below five years infected with parasites acquire malnutrition or other forms of immunosuppression that sometimes terminate in death from wasting or dehydration[3]. The majority of human disease casesare caused by the *Cryptosporidium hominis*(*C.hominis*),but the substantial disease is caused by zoonotic *Cryptosporidium parvum* (*C.parvum*) and

occasionally by other species[4].*Cryptosporidiumspp*. are declared the most widespread diarrheal pathogens worldwide.In developing nations, approximately 20 % of diarrheic children are affected by cryptosporidiosis compared to 1% to 5 % in Europe and North America[5].The developing nations have insufficientdrinking water and sewage disposal networks, so cryptosporidiosis prevalence is higher in rural areas and during the rainy season. HIV/AIDS, Malnutrition, and any immunocompromising disorders considerably upsurge the severity, risk, and prevalence of cryptosporidiosis[6]. The residential surfaces, food, and water contaminated by *Cryptosporidium* -containing feces serve as infection sources. Whenever the chain of personal hygiene breaks,person-to-person transmission is also detected.In developed nations,the transmission is to a lesser extentprobable because of public health interventions related to clean food,water treatment,and sanitation. The disease is transmitted by food-borne,waterborne, person-to-person, and zoonotic transmission pathways[5].

Still, now the healthcare system lacks highly effective treatment options. The sporulated oocysts, the disease transferring agents involved in the transmission, is highly resistant to standard water treatment methods like chlorination.Nitazoxanide is moderatelyeffective in immunocompetent patients. Thus the deterrence of infection is significant for persons with HIV/AIDS.

The theoretical and computational approaches are routinely exploitedto identify novel 'lead 'or'hit' compounds against a selected target macromolecule, and all these related disciplines are known as the computer-aided drug design (CADD) approach. The pharmacophore modeling, high throughput virtual screening, molecular docking, and molecular dynamic simulations are various feathers in the cap of CADD widely exploited to discover, develop and analyze ligand/drug and similar biologically active molecules. The molecular docking approach is used for observing the binding affinity of the compound library within the specified active-site of a target macromolecule. The docking approach helps reducethe cost and time associated with the in-vivo evaluation of a compound's biological activity with a selected target macromolecule. The pharmacological (absorption, adsorption,metabolism,excretion,toxicity, or ADMET) profile and pharmacokinetic profile can also be forecast using the CADD approach[7].

The present research relies on CADD processes like structure-based drug designingmodeling,high-throughput virtual screening, ADMET, and molecular docking approaches to identify the possible antagonist against cyclin proteins to treat cryptosporidiosis.

The phosphorylation of protein is the chief reversible process at the stage of post-translational modification (PTM). Phosphorylation of proteins is the essential and significant cellular process for regulating protein function and signal transduction throughout the cell. Although prokaryotic cells also regulate their function through phosphorylation,phosphorylation is more pervasive in eukaryotic cells. The protein phosphorylation is a reversible reaction in which the threonine, serine, and tyrosine residues are phosphorylated. The Adenosine triphosphate (ATP) acts as a universal phosphoryl group donor in phosphorylation. Phosphorylation plays a significant role in the regulation of cell growth, cell cycle, and apoptosis processes. The findings of the Human Genome project show that about 30 % of human proteome experiences phosphorylation. However, phosphorylation is a predominant PTM for the regulation of protein function. The side chains of threonine (Thr), serine (Ser), and tyrosine (Tyr) act as a site of phosphorylation. The Ser, Thr and Tyr amino acids possess a nucleophilic (-OH) group that attacks the terminal phosphate group (γ-PO_3^{-2}) on ATP, resulting in the phosphoryl relocation group from ATP to side chains of amino acids. This relocation is facilitated by magnesium (Mg^{2+}), which chelates the γ- and β-phosphate groups. The relocation of the phosphoryl group helps in dropping the threshold energy of the reaction. A large amount of free energy is released when the phosphate–phosphate bond is broken in ATP, forcing this reaction in a unidirectional way[8].

The phosphorylation also changes the conformation of proteins synonymous with change function (either activated or deactivated) and a protein's catalytic activity. The phosphorylated proteins recruit neighboring proteins that possess structurally conserved domains to bind with 'phosphomotifs' of phosphorylated proteins. These phosphodomains are amino acid-specific. For example, Src

homology 2 (SH2) and phosphotyrosine binding (PTB) domains show specificity for phosphotyrosine (pY). The Phosphoserine (pS) recognition domains include MH2 and the WW domain, while forkhead-associated (FHA) domains recognize phosphothreonine (pT). The ability of phosphoproteins to recruit other proteins is critical for signal transduction, in which downstream effector proteins are recruited to phosphorylated signaling proteins. The kinases and phosphatasescatalyzeproteins' phosphorylation, catalyzing phosphorylation and dephosphorylation ofproteins, respectively[9].

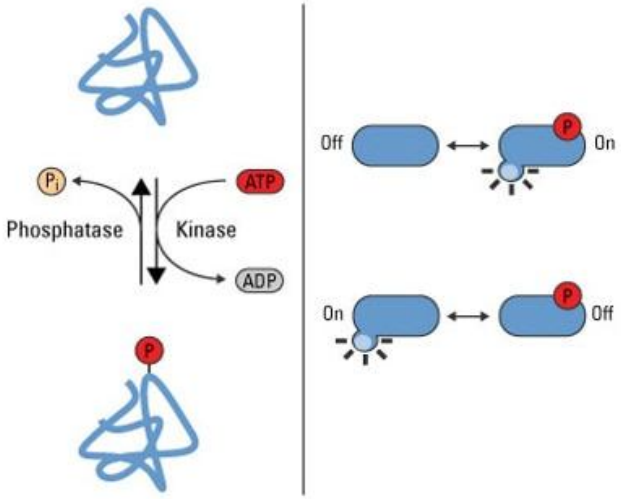

Figure1: The Diagram showing phosphorylation as a reversible PTM that regulates protein function. Phosphorylation causes conformational changes in proteins that either activate or inactivate protein function (adapted from Thermo Scientific Books on Protocol)

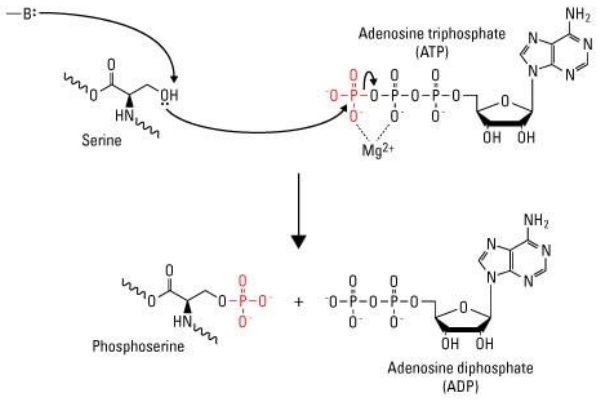

Figure 2: Diagram of serine phosphorylation. Enzyme-catalyzed proton transfer from the (-OH) group on serine stimulates the nucleophilic attack on the γ-phosphate group on ATP, resulting in the transfer of the phosphate group to serine to form phosphoserine and ADP

2.MATERIAL AND METHODS

2.1:Sequence Retrieval and three-dimensional (3D) structure prediction: The primary amino acid sequence of cyclin-dependent kinase 1 of *Cryptosporidium parvum* (accession number:XP_001388101.1) was retrieved from NCBI database (https://www.ncbi.nlm.nih.gov/) in FASTA format[10].

2.2.Target protein model generation and validation: The BLAST analysis was performed over CpCDK1 protein with all default parameters against all structures deposited in PDB (https://www.rcsb.org/)[11]. The BLAST analysis of CpCDK1) revealedthat the crystal structure of activated calcium-dependent protein kinase 1(CpCDK1 from *Cryptosporidium parvum* (PDB ID:3MWU) has 90 % identity, so this protein is used as a template input for homology modeling[12]. I-TASSER (https://zhanglab.ccmb.med.umich.edu/I-TASSER/), the tool was deployed for the 3D model of target protein generation. The all the generated model was thoroughly analyzed, and the best model was picked for the other structure validation process[13].

2.3: High-Throughput virtual screening: Virtual screening isan indispensable tool for recognizing 'leads' among millions of compounds, available in the form of databases. The identified leads act as a starting point for in-silico drug designing projects saving cost and time involved in drug designing and discovery projects. The Zinc

Database (http://zinc12.docking.org/) is deployed for virtual screening of leads against CpCDK1 protein using the AutoDock Vina(http://vina.scripps.edu/) tool[14][15]. The lead-like subset was downloaded in SDF format and converted to mol2 format through the Open Babel tool. The MMFF94 force field was used for the energy minimization of generated conformer. All the compounds with binding energy (-7.0 Kcal/mol) more significant than reference value were selected and submitted for the second round of molecular docking analysis.

2.4:Pharmacokinetics profile analysis: The toxicity analysis is an essential pharmacodynamics analysis. It summarizes the toxicity effects of a compound in the human body. The Swiss ADME tool was deployed for the toxicity analysis of selected compounds after docking simulation[16].

2.5: Molecular Docking Analysis: Theselected hit molecules from the first round of docking were submitted tothe second round of molecular docking simulation using the AutoDock Vina tool. The AutoDcok is the most popular,efficient, and robust tool for docking analysis. The CDPK1 protein and the selected lead compounds were prepared for docking analysis. A grid box of 5 Å is created around the potential active site of the protein. Based on the known active-site residues, the grid box was adjusted. The default parameters of AutoDock was used for complete docking analysis, and the best 50 docking complex for each hit compound was generated. The other selection of compounds is made based on docking energy. All the compounds having docking energy higher than the reference ligand docking energy are chosen for further analysis.The potential ' lead ' compound was selected based on the binding affinity (higher than reference ligand) and binding mode[7].

3.RESULT AND DISCUSSION

3.1 Target protein selection and Model validation: The CpCDK1 proteins are the serine/threonine kinase family's unique protein present in apicomplexan protozoa, including C. parvum. The CpCDK1 participates an exclusive role in calcium-dependent cell signaling almost in all sexual stages of the parasite. The CpCDK1 are potential drug targets as there are no CpCDK1 orthologous in the host human. The kinases genes. The group members are CaMK, AGC, Atypical, CMGC, CK1, and TLK. About 35 % of these proteins are grouped as Other Protein Kinases (OPK), and 25 %of these OPK did not have any known orthologues in humans. In previous studies, it has been proven that unique assemblies of amino acid residues act as 'gatekeepers' at the hinge region of the protein. These gatekeeper residues, the hydrophobic pocket that accommodates ATP purine ring during phosphoryl group transfer, become enlarged. This unique structural property of CpCDK1 could be exploited for drug discovery projects. The CpCDK1 plays a role in cell cycle control, and their inhibition could interfere with the parasite growth and proliferation. The CpCDK1 displays significant divergence from the host counterpart, so these evolutionary and structural characteristics of CpCDK1 are exploited here for selective anti-cryptosporidial drug development. The PROCHEK (https://www.ebi.ac.uk/thornton-srv/software/PROCHECK/) tool was used for protein structure validation[17]. The atomic coordinates of the selected modeled protein were uploaded in PROCHECK for the overall quality assessment of the model. The Z-score represents a value that represents the ranges of scores typically found for native proteins of similar size. The z-score of the submitted model is -9.39, which is in the permissible range and shown in figure 3.

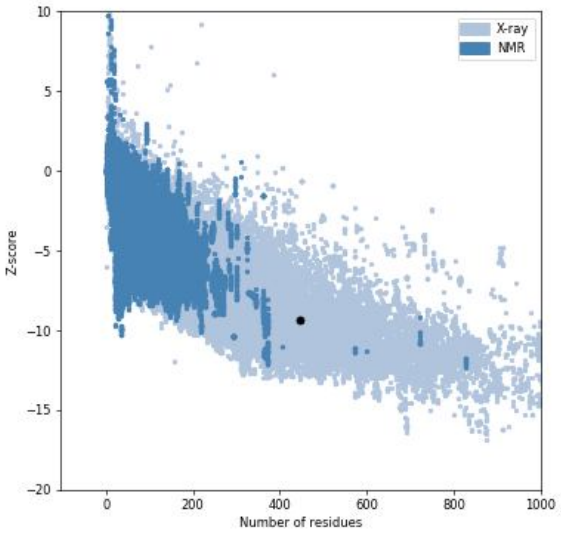

Figure 3: Different colors distinguish the Z-score plot of the modeled protein structure. In this plot, the groups of structures from different sources (X-ray, NMR).

The modeled protein structure was submitted to EDS (http://eds.bmc.uu.se/eds/) server for the quality assessment and results shown in Table 1. The EDS help in crystallographic data analysis of modeled protein as well as structures deposited in the PDB. Most of the parameters are in the range, proving that the protein's selected model is validated.

Table 1: The Electron Density Server Summary report of modeled protein structure.

Electron Density Server Summary	
Map status	CCP4
Resolution from map calculation	42.04-1.99 Å
Resolution from PDB header	1.98 Å
R-value for map	0.203
R-value (free R) from PDB header	0.196 (0.229)
Completeness of data	99.8 %
Cell dimension	a=60.02 Å, b=55.97 Å, c=82.21 Å alpha=90.00,beta=104.79, gamma=90.00
Number of reflections	36125
Correlation coefficient F_o and F_c	0.954
Wilson Plot B -factor	37.1 $Å^2$
Bulk -solvent scale factor (k)	0.316 e/ $Å^3$
Bulk solvent B -factor	44.2 $Å^2$
Number of non-hydrogen atoms	3661plus 161 hetero atoms
Mean (Standard Deviation) for non-water residues	
Real- space R-value	0.163(0.093)
Real -space correlation coefficient	0.914 (0.098)
Occupancy- weighted average temp factor	67.3 (29.6) $Å^2$

The Ramachandran plot analysis of these modeled structures shows that the number of outliers for this modeled protein is 13, and outlier percentages are 3 % in the permissible range. The Ramachandran plot is shown in figure 4.

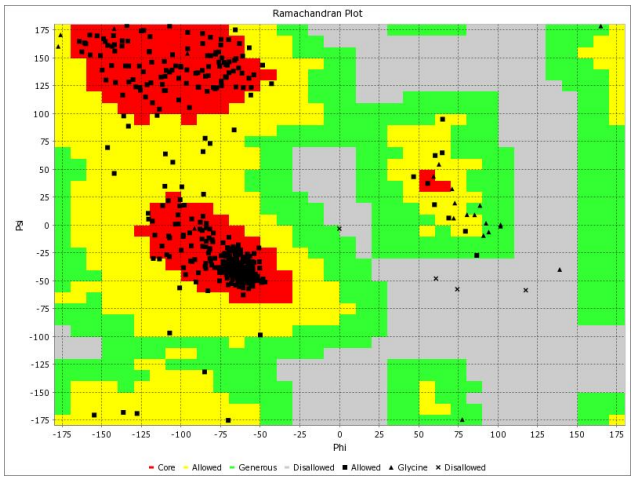

Figure 4: The Ramachandran Plot of modeled protein structure

Finally, the modeled protein structure is submitted to the VADAR (http://vadar.wishartlab.com/cgi-bin) server for overall 3D model structure validation. The VADAR (volume, area, dihedral angle reporter) is a compilation of more than 15 algorithm s and programs for analyzing and assessing peptide and protein structure. The output is in the form plot, which shows each amino acid residue's conformational position and shown in figure 5. Most of the residues are in the favorable region, so the model of the protein is correct. The 3D structure of a modeled protein is shown in figure 6.

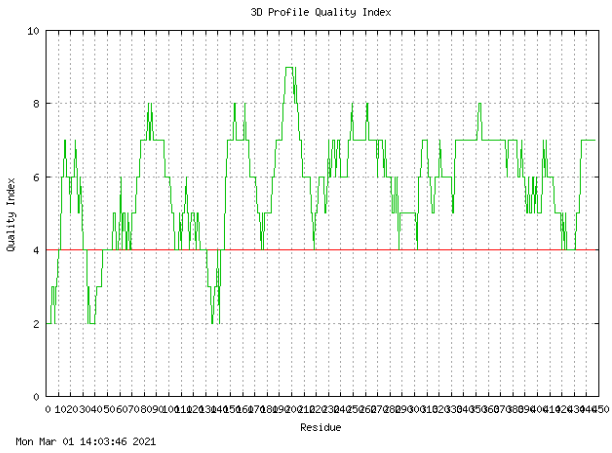

Figure 5: The 3D profile quality index of modeled protein structure

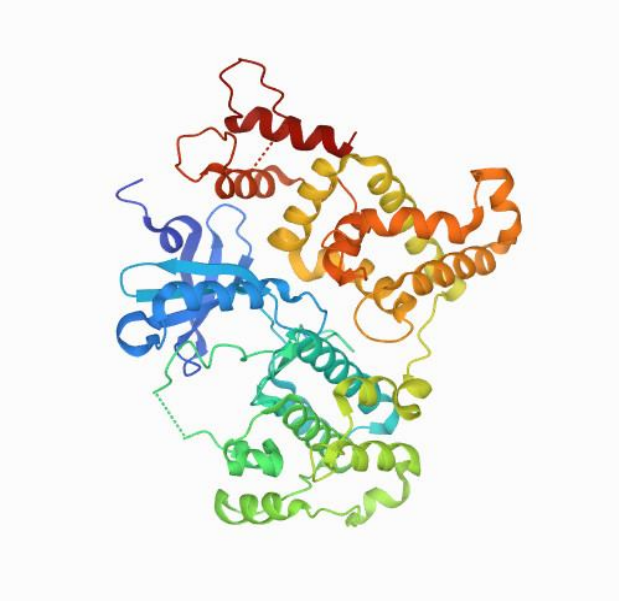

Figure 6: The 3D structure of the modeled protein.

3.2: High- throughput virtual screening: For high throughput virtual screening, we used the lead-like subset of the ZINC database. This subset contains 6,05,3,287 compounds.These compounds were first sorted out based on drug-likeness properties defined by Lipinski rule of five and SwissADME filter. After this,a manual inspection was performed over the compound library to discard any disordered compound. The remaining (1000) compounds that cross above mentioned filter were docked to CpCDKI (PDB ID: 3MWU) protein and sorted based on binding energy. The top 100 'hits' having higher binding energy than the reference ligand was chosen.

3.3: Molecular Docking Analysis: To understand the binding interactions of ligands into the active-site of CpCDK1 and assist the recognition of novel inhibitors against CpCDK1, the active-site binding mode of calcium-dependent protein kinase 1 from *Cryptosporidium parvum* with inhibitor (BK3) was examined. Initially, molecular docking analysis was performed to carry out binding mode analysis of BK3 in the active-site of 3MWU. The best-docked conformation of BK3 showed hydrogen bonding interactions with the Glu153, Tyr 155, and Glu159 amino acid residues with a binding free energy -7.0 kcal/mol.

The docking simulation of CpCDKI and top 100 hits was performed using the AutoDock Vina tool. The binding modes for the 100 hits identified by virtual screening were ranked according to the binding energy constraints. After visual inspection,the most favorable (top 10 %)'leads' with the best binding modes and structural diversity were selected. The 3-(naphthalen-1-ylmethyl)-1-(piperidin-4-ylmethyl)-1H-pyrazolo [3,4-d] pyrimidin-4-amine (BK3), a known inhibitor of CpCDK1, was used to comprehend the molecular -recognition interactions employing molecular docking analysis. This analysis helped in validating the computational protocol and established the participation of Glu159, Leu205, Glu202, Leu154, Ala103, Asp219, Lys105, Glu153, Ile150, Tyr153, Leu82, Val90, Leu138, Met136, and Ala183 amino acid(AA) as the key AA in stabilizing ligand-protein interactions for effective binding along with the involvement of three hydrogen-bond interaction. A total of 13 leads or compounds shown good binding free energy as wellthe required hydrogen bonding interaction with the active-site residues. All these 13 compounds inhabited the area on the verge of the active-site of CpCDK1 and showed consistency in docking simulations. Although these compounds are not derivative of BK3 but have a similar structure with variant side-chain group, hence they can be for CpCDK1 inhibitors. The results are exciting and help to justify the high potential 'lead' compounds for drug designing against CpCDK1 to treat cryptosporidiosis.

Table 2: List of screened molecules after high-through put virtual screening, Lipinski rule of 5, ADMET parameter and molecular docking studies using 3MWU template withinteracting amino acid residues.

S.No.	Compound ID	Estimated Free Energy Of Binding (Kcal/Mol)	Estimated Inhibition Constant Ki(μM)	VdW + H-Bond + desolvation Energy (Kcal/mol)	Electrostatic Energy (Kcal/Mol)	Total Inter molecular Energy (Kcal/Mol)	H-Bonding AA Residues	Polar Bonding AA Residues	Hydrophobic Bonding AA Residues	Other Bonding AA Residues
1	22989113	-6.5	17.29	-6.21	-2.23	-6.88	GLU153,TYR155,GLU159	LEU205,GLU202,LEU154	MET136	ASP219,ALA103,GLU153,ILE150,TYR153,LEU82,VAL90,LEU138,MET136
2	23655590	-5.81	55.38	-5.49	-0.28	-5.77	SER48,ASP252,MET273,SER276	SER48,ASP219TYR155	MET50,MET136	SER48,ALA49,MET50,LYS210,ASP252,MET273
3	12310311	-6.2	28.38	-6.16	-0.14	-6.3	MET50,GLU159,TYR155,GLU153	ASP219,LYS105,ILE150,TYR153	MET136	LEU205,ASP219,LEU154,LEU82
4	23616521	-6.12	32.46	-6.5	-0.23	-6.73	TYR155,LYS210,ILE255,SER276,GLU153,GLU159	SER48,ASP153,ASP252,SER276,GLU202,ALA103	MET50	SER48,MET50,ASP252,ILE255,MET273,SER276,LEU183,VAL90,LEU138
5	8339	-6.18	29.34	-6.49	-0.26	-6.74	,LYS210,ILE255,GLU159,TYR155	SER48,ASP163,ASP252,VAL90	MET50	SER48,MET136,ASP252,ILE150MET273,ILE276,SER276
6	1549076	-6.11	33.05	-6.49	-0.45	-6.94	GLU153,GLU159,ASP252,MET273,SER276,TYR155	SER48,ASP163,LYS210,ASP252,GLU159,LEU205,GLU202,LEU154,ASP219	MET50,MET136	LYS105,LEU154,GLU153,ILE150,LEU82
7	1549079	-6.11	33.05	-6.49	-0.45	-6.94	GLU153,SER276,GLU159	SER48,ASP163,LYS210,ASP252	MET50,MET273	SER48,ALA49,MET50,ASP163,LYS210,ASP252,SER276
8	4275593	-6.42	19.6	-6.32	-0.33	-6.55	GLU153,ILE255,MET273,TYR155,GLU159	SER48,ASP163,ASN191,LYS210,ASP252,SER276	ILE255	SER48,MET50,ASP163,ASN191,ASP252,ILE256,SER276,ILE274,MET273
9	445057	-6.28	24.97	-4.87	-0.02	-4.89	SER48,MET273,TYR155,SER276,GLU153,GLU159	LYS210,ASP252,SER276	MET50	SER48,MET50,ASP252,ILE255,MET273,SER276
10	5326975	-6.31	23.71	-6.8	-0.43	-7.24	LYS210,ILE255,MET273,SER276,GLU153,GLU159,TYR153	SER48,ASP163,ASP252,SER276	ILE255	SER48,ALA9,MET50,SER276,ASP163,ASP252,ILE255,ILE274
11	57017947	-6.5	17.22	-6.72	-0.27	-6.99	SER48,GLY275,SER276,GLU153,GLU159,TYR155	SER48,LYS210,ASP252,SER276	MET136,MET50	SER48,ALA9,MET50,LYS210,ASP252,MET273,SER276
12	92209828	-6.34	22.39	-5.89	-0.12	-6.01	Met273,GLU159,TYR155	SER48,ASP252,SER276	MET50,MET136	SER48,MET136,ASP219,ILE150,MET273,SER276,ASP219
13	10635051	-5.78	57.7	-5.69	-0.36	-6.05	SER48,MET273,SER276,GLU153,GLU159,TYR155	SER48,ASP252,SER276.ASP219,LYS105,LEU154,GLU202,LEU205,GLU159	MET136,ILE255	GLU153,MET136,VAL90,LEU138,TYR155
14	BK3 (reference ligand)	-7.1	161.47	-5.67	-0.03	-7.68	GLU153, TYR155,GLU159	GLU159,ILE205,GLU202,LEU154,ALA103,ASP219,LYS105,LEU154	MET136	GLU153,ILE150,TYR155,LEU82,VAL90,LEU138,MET136,ALA103

* AA - Amino Acid

* VdW - Van der Waals Energy

* H-Bond - Hydrogen Bond

4.CONCLUSION

How can we undertake the global threat of COVID-19 without neglecting the fight against cryptosporidiosis? The present research investigation shed light on how to effectively combat the diarrhea-endemic world's dual challenges alongside unexperienced problems presented by the COVID-19 pandemic. We must tackle these global health challenges together as a united community to not lose ground against either of these formidable diseases.

In the present research investigation, the CpCDK1 protein was employed as an appropriate target for anti-cryptosporidial drug development. The genomic sequence of the protein is retrieved from NCBI, and a 3D model of the protein is generated using I-TASSER tool. The selected model is analyzed, tested, and validated by different in-silico tools.the detailed annotation of CpCDK1 protein shown that structurally and functionally, CpCDK1 belongs to the CDK family. The Zinc database's lead-like subset was deployed for the identification of potential lead compounds against

CpCDK1 proteins. The AutoDock 4.2 was deployed forVirtual screening andcritical binding interaction analysis of finally selected lead molecules. Furthermore, the best-docked compounds supplied with essential binding residues and binding energy were considered as potential anti-CpCDK1 lead compounds. The best compound identified was considered as 'lead' for further in-vitro analysis.

CONFLICT OF INTEREST

The authors declare no conflict of interest, financial or otherwise.

ACKNOWLEDGEMENT

Declared none.

REFERENCES

[1] A. Efstratiou, J. E. Ongerth, and P. Karanis, "**Waterborne transmission of protozoan parasites: Review of worldwide outbreaks - An update 2011–2016,**"*Water Research*, vol. 114. 2017, doi: 10.1016/j.watres.2017.01.036.

[2] U. Ryan, A. Zahedi, and A. Paparini, "**Cryptosporidium in humans and animals—a one health approach to prophylaxis,**"*Parasite Immunology*, vol. 38, no. 9. 2016, doi: 10.1111/pim.12350.

[3] H. Sparks, G. Nair, A. Castellanos-Gonzalez, and A. C. White, "**Treatment of Cryptosporidium: What We Know, Gaps, and the Way Forward,**"*Current Tropical Medicine Reports*. 2015, doi: 10.1007/s40475-015-0056-9.

[4] W. Checkley *et al.*, "**A review of the global burden, novel diagnostics, therapeutics, and vaccine targets for cryptosporidium,**"*The Lancet Infectious Diseases*. 2015, doi: 10.1016/S1473-3099(14)70772-8.

[5] B. Shah, P. Modi, and S. R. Sagar, "**In silico studies on therapeutic agents for COVID-19: Drug repurposing approach,**"*Life Sci.*, 2020, doi: 10.1016/j.lfs.2020.117652.

[6] A. Morris, J. Pachebat, G. Robinson, R. Chalmers, and M. Swain, "**Identifying and resolving genome misassembly issues important for biomarker discovery in the protozoan parasite, cryptosporidium,**" 2019.

[7] S. P. Leelananda and S. Lindert, "**Computational methods in drug discovery,**"*Beilstein Journal of Organic Chemistry*. 2016, doi: 10.3762/bjoc.12.267.

[8] P. Cohen, "**The regulation of protein function by multisite phosphorylation–a 25 year update,**"*Trends Biochem. Sci.*, vol. 25, no. 12, pp. 596–601, 2000.

[9] F. Ardito, M. Giuliani, D. Perrone, G. Troiano, and L. Lo Muzio, "**The crucial role of protein phosphorylation in cell signaling and its use as targeted therapy,**"*Int. J. Mol. Med.*, vol. 40, no. 2, pp. 271–280, 2017.

[10] D. L. Wheeler *et al.*, "**Database resources of the National Center for Biotechnology Information,**"*Nucleic Acids Res.*, 2008, doi: 10.1093/nar/gkm1000.

[11] Y. Huang, B. Niu, Y. Gao, L. Fu, and W. Li, "**CD-HIT Suite: A web server for clustering and comparing biological sequences,**"*Bioinformatics*, 2010, doi: 10.1093/bioinformatics/btq003.

[12] M. Johnson, I. Zaretskaya, Y. Raytselis, Y. Merezhuk, S. McGinnis, and T. L. Madden, "**NCBI BLAST: a better web interface.,**"*Nucleic Acids Res.*, 2008, doi: 10.1093/nar/gkn201.

[13] J. Yang, R. Yan, A. Roy, D. Xu, J. Poisson, and Y. Zhang, "**The I-TASSER Suite: protein structure and function prediction,**"*Nat. Methods*, vol. 12, no. 1, pp. 7–8, 2015.

[14] J. J. Irwin and B. K. Shoichet, "**ZINC - A free database of commercially available compounds for virtual screening,**"*J. Chem. Inf. Model.*, 2005, doi: 10.1021/ci049714+.

[15] O. Trott and A. J. Olson, "**Software news and update AutoDock Vina: Improving the speed and accuracy of docking with a new scoring function, efficient optimization, and multithreading,**"*J. Comput. Chem.*, 2010, doi: 10.1002/jcc.21334.

[16] N. Guex and M. C. Peitsch, **"SWISS-MODEL and the Swiss-PdbViewer: An environment for comparative protein modeling,"** *Electrophoresis*, 1997, doi: 10.1002/elps.1150181505.

[17] R. A. Laskowski, M. W. MacArthur, and J. M. Thornton, **"PROCHECK : validation of protein-structure coordinates ,"** 2012.